One-dimensional alignment of nanoparticles via magnetic sorting

R. Bouskila,[1] R. McAloney,[2] S. Mack,[3] D. D. Awschalom,[3] M. C. Goh,[3] and K. S. Burch[3,a)]
[1]*Department of Physics, Institute of Optical Sciences, University of Toronto, 60 St. George Street, Toronto, Ontario M5S 1A7, Canada*
[2]*Department of Chemistry, Institute of Optical Sciences, University of Toronto, 80 St. George Street, Toronto, Ontario M5S 3H6, Canada*
[3]*Center for Spintronics and Quantum Computation, University of California, Santa Barbara, California 93106, USA*

(Received 21 February 2010; accepted 1 April 2010; published online 19 April 2010)

Near room temperature, MnAs films align into two phases, one ferromagnetic and the other paramagnetic. These phases take the intriguing form of nanoscale wires. We have exploited this phase coexistence to form linear arrays of magnetite nanoparticles without the need for photolithography. This is confirmed via extensive scanning probe microscopy. © *2010 American Institute of Physics*. [doi:10.1063/1.3405732]

Many research groups have recently turned their attention to the problem of forming linear patterns of nanoscale particles.[1–8] Such arrays are of interest for studies of the effects of low dimensionality on the electronic, magnetic, and optical properties of materials, as well as for applications such as biological and chemical sensing.[9,10] The dominant paradigm is to fabricate a template along which the nanoparticles will subsequently self-assemble along. This method, although successful, tends to be an expensive, complex process.[9] In this study, we have exploited the naturally-occurring magnetic order of MnAs thin films as a template for forming linear arrays of magnetite (Fe_3O_4) nanoparticles.

Bulk MnAs is ferromagnetic at low temperatures (α phase) but undergoes a first-order magnetic and structural phase transition at ≈318 K to the β phase. This phase transition results in a reduction in the a-axis lattice constant and a spontaneous loss of magnetization.[11] For the past decade there has been renewed interest in MnAs, as thin films can be grown on GaAs and Si substrates via molecular beam epitaxy.[12–15] These films, originally developed for applications in spintronics and magnetic storage, behave quite differently from the bulk material. Indeed strain due to the substrate causes the film to form alternating linear domains of ferromagnetic α phase and paramagnetic β phase. These domains are almost invisible to a topographical study such as atomic force microscopy (AFM) but show up in high relief in a magnetic force microscopy (MFM) scan.[13] We have successfully exploited these linear domains to trap magnetite nanoparticles into one-dimensional arrays. This is confirmed via analysis of combined MFM and AFM studies.

A 60 nm film of MnAs was grown on a semi-insulating GaAs(001) substrate, as detailed in Ref. 13. In Fig. 1(a) we present a 296 K AFM scan of our film before deposition of the nanoparticles. It is quite flat (rms roughness of 2.3 nm), aside from small particulates on the surface of the film, and two scratches crossing it. Furthermore, the fast Fourier transform (FFT) of the AFM data [Fig. 1(c)] reveals no evidence of ordering peaks; confirming our assertion that the AFM is not sensitive to the phase separation. Turning to the MFM image shown in Fig. 1(b), we show the change in the phase of the cantilever motion. This change in phase results from the force exerted on the cantilever by the stray magnetic fields of the film. In this image the one-dimensional alignment of the α and β phases is clear, and is consistent with previous studies.[14,15] The FFT of the MFM data shown in Fig. 1(d) reveals two clear peaks due to the phase separation. For the most part the MFM data is unrelated to the topography, except for some distortion around dust particles. This indicates that we can separately evaluate the existence of additional particles on the surface from the underlying magnetic ordering of the MnAs film.

Colloidal nanoparticles of magnetite and titania (TiO_2, a nonmagnetic control) were provided by Vive Nano, Inc. These nanoparticles are 10 nm in diameter, and are surrounded with a small sphere of remanent colloid.[16] The particles were prepared in a solution of 0.01 M sodium hydroxide and sonicated for 30 s to prevent the formation of aggregates. Next a single drop of the nanoparticle solution was deposited on the MnAs film. As MnAs is a hydrophobic surface, the solution formed a bead upon deposition. A 30 s settling period was allowed so that the nanoparticles would find a local energy minimum via Brownian motion. Finally, the bulk of the solution was removed by wicking with wiping paper, leaving a thin film behind, which was dried in air.

After deposition, the films were imaged using a Digital Instruments scanning probe device. We used magnetized

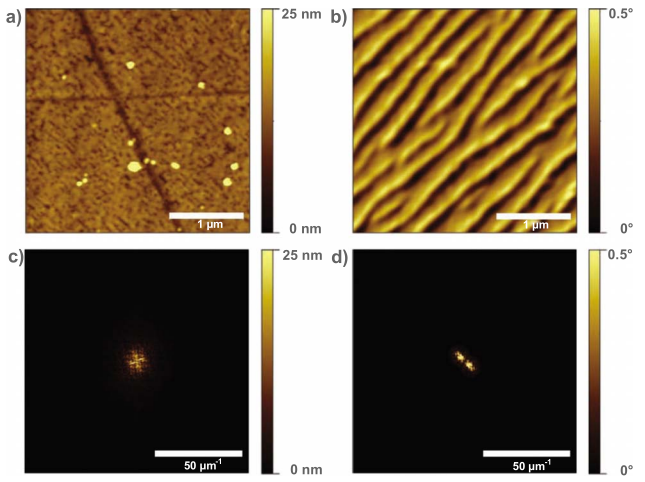

FIG. 1. (Color online) MnAs film grown on GaAs. (a) Topography of the film with an rms roughness of 2.3 nm, (b) Magnetic field gradient measured with the AFM data; (c) FFT of the data in (a), with no evidence for order, (d) FFT of the data in (b), with two peaks due to the stripes.

a)Electronic mail: kburch@physics.utoronto.ca.

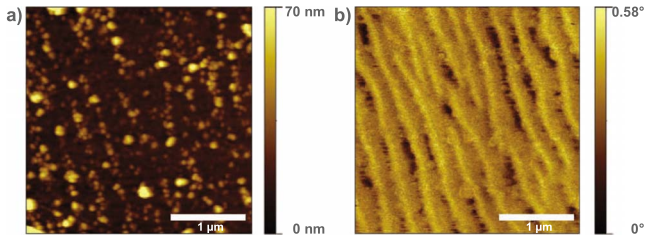

FIG. 2. (Color online) 4×4 μm^2 scans of Fe_3O_4 nanoparticles on MnAs film. (a) AFM data showing the linear alignment of the nanoparticles, (b) MFM data replace with: confirming alignment of the nanoparticles follows the magnetic order.

Veeco (model MESP) probes to perform MFM measurements interleaved with atomic force imaging.[17] The TappingMode™ AFM image revealed the surface topography and the rest positions of the settled nanoparticles, whereas the magnetic force image, taken at a lift height of 30 nm, revealed the orientation and location of the MnAs magnetic domains.

The nanoparticles appear in the AFM micrograph in Fig. 2(a) as approximately 10 nm increases in the height of the surface, with a circular diameter of approximately 50 nm. There is an apparent linear alignment of the particles. It bears note that although the diameter of the actual particles is very small, upon deposition their colloidal coating flattens out to a much wider diameter. This is evident in the circular diameter of the particles seen in the AFM micrographs. The existence of this colloid also makes it difficult to determine the exact position of the nanoparticle. Nonetheless, it is worth comparing the AFM data shown in Fig. 2(a) with the underlying magnetic domain structure as shown in the MFM image [Fig. 2(b)]. A cursory examination of these two figures clearly shows the direction of alignment of the nanoparticles closely follows the orientation of the nanowires in the film.

This alignment exists over large distances, as seen in Fig. 3, where we present a second sample, with a much wider scan size (10×15 μm^2). To confirm the alignment of the Fe_3O_4 nanoparticles matches the MnAs nanowires we exploit the wealth of information provided by the FFT. Indeed, from the FFT we can establish the periodicity, direction, and correlation length of the magnetic domains and lines of nanoparticles. We wish to quantifiably determine whether the periodicity and direction of the lines of nanoparticles is the same as the MnAs domains.

The FFTs of the AFM and MFM data presented in Figs. 3(a) and 3(b) can be seen in Figs. 3(c) and 3(d), respectively. For linear patterns, the FFT includes two peaks whose centers are equally spaced from q=0, and lie along the axis of modulation (i.e., transverse to the lines). These peaks are clearly visible for the magnetic domains in MnAs [cf. Fig. 3(d)] but for a more complex structure, additional features can arise making the peaks more difficult to detect. Nevertheless, corresponding modulation peaks exist in both FFT images. Indeed, both Figs. 3(c) and 3(d) include two bright peaks at $q=\pm3.1$ μm^{-1}, indicating that the direction and period of the linearly ordered particles closely matches the underlying magnetic order of the MnAs film.

To confirm the alignment is due to the underlying magnetic order, the process described above was repeated using nonmagnetic TiO_2 nanoparticles. The results of this experiment are presented in Fig. 4. The MFM image [Fig. 4(c)] displays a vertical ordering, which is not apparent in the AFM image [Fig. 4(a)]. The unordered state of the TiO_2 control is a strong indication that the ordering seen with magnetite particles is due to the high magnetic permeability of the magnetite particles, rather than the surface topography.

We have evaluated the results presented in Figs. 3(b) and 3(d) by fitting each peak with two Guassians of width Γ_1 (width along the ordering vector) and Γ_2 (width normal to the ordering vector). The results of these fits are presented in Table I. The FWHM of the Gaussian in the direction of the line between the two peaks (Γ_1), gives a measure of the variance in the spacing of the stripes, whereas Γ_2 gives a measure of the variance in the length of the stripes. These are the inverses of the correlation lengths in the direction of modulation (i.e., over what distance the lines keep the same modulation period) and in the perpendicular direction (i.e., how long the stripes tend to be). The results presented in Table I indicate the period and correlation lengths for the MFM and AFM data are essentially the same. This result and the lack of ordering for the TiO_2 particles (see Fig. 4), strongly suggest the linear alignment of the Fe_3O_4 nanoparticles results from the underlying MnAs magnetic stripes.

Before concluding we discuss the mechanism by which the magnetite nanoparticles are aligned into one dimensional wires. Preliminary magnetic susceptibility measurements of the Fe_3O_4 particles indicate they are superparamagnetic at 296 K with a specific magnetization (σ) of 4–10 emu/g. The potential energy (U) for these particles in the field produced by the MnAs film ($\vec{B}$) is $U=-\vec{m}\cdot\vec{B}$. Since our experiments are performed with the particles in solution at 296 K, we expect the direction of the magnetic moment ($\vec{m}$) to be easily rotated. Therefore the direction $\vec{m}$ will closely follow that of

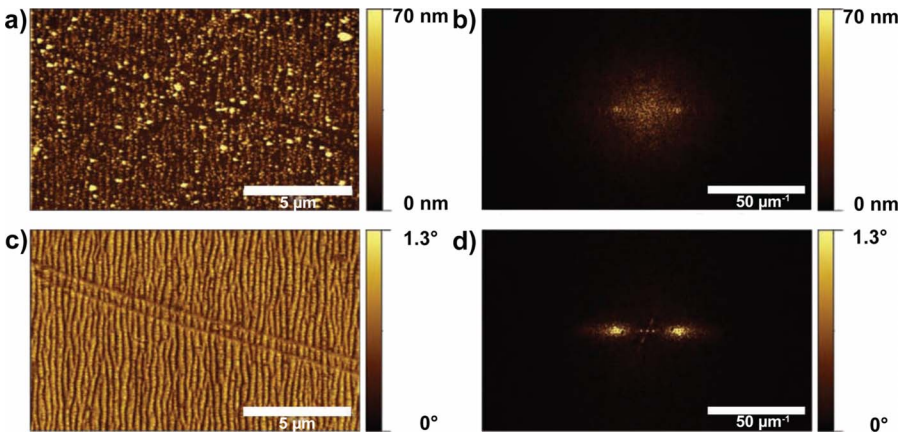

FIG. 3. (Color online) 10×15 μm^2 scans revealing long range alignment. (a) Topography data with (b) Fourier transform of the data presented in (a). The alignment results in two peaks in the FFT; (c) MFM, showing underlying MnAs domains, with (d) the Fourier transform of (c). The peaks in (d) match those of (b) confirming the dots line up with the MnAs domains.

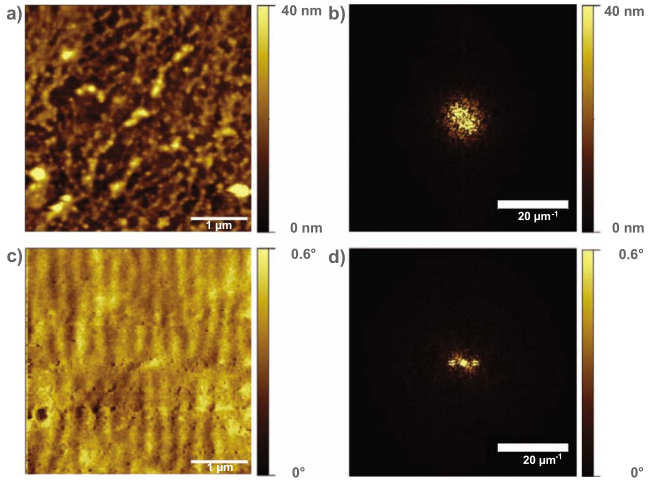

FIG. 4. (Color online) TiO_2 nanoparticles on MnAs. (a) AFM, revealing no nanoparticle alignment, (b) FFT of the data in (a), (c) MFM, showing MnAs domains, (d) the Fourier transform of (c) confirming domain alignment. Taken together this shows the film magnetic order did not affect the nanoparticles deposition.

$\vec{B}$ so long as the magnetic field orientation changes slowly compared to the velocity of the particles. As a result, the particles should be trapped in regions with a high magnetic field. To determine the strength of $|\vec{B}|$ we conducted a finite-element method simulation (via the software COMSOL MULTIPHYSICS) of the magnetic fields due to the MnAs film. The strength of the field from these simulations is shown in Fig. 5.

From the results presented above, it is apparent that the locations where the magnetic field is highest lie at the domain walls between the α and β phases. To determine whether the potential generated by this field is strong enough to trap the particles, we treat them as point like particles with total $|\vec{m}|=(4\pi/3)r^3\rho\sigma$; where r is the radius (5 nm) and ρ the density of the nanoparticles (taken to be the same as bulk Fe_3O_4: 5.15 g/cm^3). Next we set $|\vec{B}|=0.3$ T from the simulation results at a height of 5 nm (radius of the nanoparticles) above the surface. This leads to a trapping potential for the magnetic nanoparticles of $U=-|\vec{m}||\vec{B}|=780\ \mathrm{K}\rightarrow 1950\ \mathrm{K}$, where this range originates from the error in $|\vec{m}|$ values of the Fe_3O_4 particles. The rather large values of the confinement potential confirm that it is the magnetic fields of the MnAs nanowires that align the magnetite nanoparticles.

Numerous applications and research possibilities present themselves for this method. The ability to trap magnetic particles and order them into linear arrays enables self-assembly of more complex molecules into such patterns via functionalization of the nanoparticles with organic ligands. Since the MnAs domain widths can be controlled via temperature, one could impose a thermal gradient on the sample prior to deposition to sort the nanoparticles by size. Lastly, the periodicity of the domains can be tuned with film thickness offering a wide degree of freedom for the nanoparticle alignment.

TABLE I. Data extracted from the FFTs in Fig. 3.

Scan	q peak (μm^{-1})	Period (μm)	Γ_1 (μm^{-1})	Γ_2 (μm^{-1})
MFM	3.10	0.322	1.32	0.397
AFM	3.11	0.321	1.45	0.361

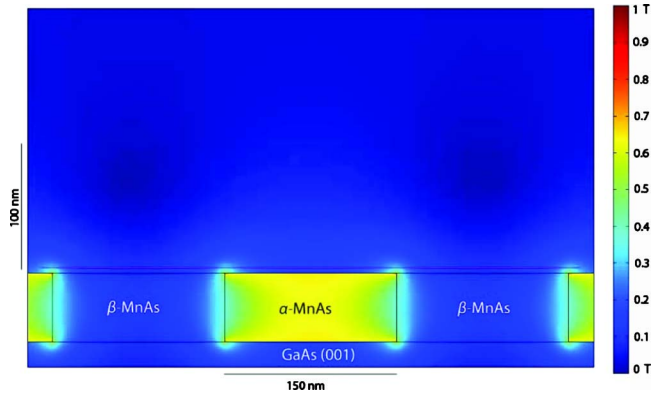

FIG. 5. (Color online) Magnetic field strength due to the MnAs film from the finite-element simulation. The line 5 nm above the surface indicates the center position of the Fe_3O_4 nanoparticles.

Another implication of this work is the detection of underlying magnetic order via deposition of magnetite nanoparticles on a substrate. Indeed we have shwon that these particles will align themselves with the underlying magnetic patterns, which could be revealed by an AFM scan. Perhaps the most promising direction of research is the investigation of arbitrary pattern formation. Indeed, one could deposit Fe_3O_4 nanoparticles upon a substrate with a predesigned magnetic field arrangement providing pattern formation without the need for a prefabricated mechanical template. As a first step to these goals, we demonstrated the formation of linear arrays of magnetite nanoparticles upon a MnAs thin film. The pattern formation relies upon the magnetic nature of the nanoparticles and the underlying magnetic order of the film. A method for the self-assembly of patterns of magnetic nanoparticles using nanoscale magnetic fields was proposed.

We are grateful for numerous discussions with A. Dattlebaum and G. Montano. Work at the University of Toronto was supported by NSERC, CFI, ORF, and OCE. Work at UCSB was supported by DARPA and ONR.

[1] S. Wirth and S. von Molnar, J. Appl. Phys. **87**, 7010 (2000).
[2] H. Li, S. H. Park, J. H. Reif, T. H. LaBean, and H. Yan, J. Am. Chem. Soc. **126**, 418 (2003).
[3] W. A. Lopes and H. M. Jaeger, Nature **414**, 735 (2001).
[4] M. G. Warner and J. E. Hutchison, Nature Mater. **2**, 272 (2003).
[5] W. A. Lopes, Phys. Rev. E **65**, 031606 (2002).
[6] D. Aurongzeb, Appl. Phys. Lett. **89**, 123128 (2006).
[7] C. Engtrakul, Y.-H. Kim, J. M. Nedeljkovic, S. P. Ahrenkiel, K. E. H. Gilbert, J. L. Alleman, S. B. Zhang, O. I. Micic, A. J. Nozik, and M. J. Heben, J. Phys. Chem. B **110**, 25153 (2006).
[8] K. Xu, L. Qin, and J. R. Heath, Nat. Nanotechnol. **4**, 368 (2009).
[9] Y. Xia, P. Yang, Y. Sun, Y. Wu, B. Mayers, B. Gates, Y. Yin, F. Kim, and H. Yan, Adv. Mater. **15**, 353 (2003).
[10] D. Horák, B. Rittich, and A. Španová, Proceedings of the Sixth International Conference on the Scientific and Clinical Applications of Magnetic Carriers (SCAMC-2006); [J. Magn. Magn. Mater. **311**, 249 (2007)].
[11] N. Menyuk, J. A. Kafalas, K. Dwight, and J. B. Goodenough, Phys. Rev. **177**, 942 (1969).
[12] B. Gallas, J. Rivory, H. Arwin, F. Vidal, and V. H. Etgens, Phys. Status Solidi A **205**, 859 (2008).
[13] M. Tanaka, Semicond. Sci. Technol. **17**, 327 (2002).
[14] A. Ney, T. Hesjedal, C. Pampuch, A. K. Das, L. Däweritz, R. Koch, and K. H. Ploog, Phys. Rev. B **69**, 081306 (2004).
[15] B. Jenichen, D. K. Satapathy, W. Braun, V. M. Kaganer, L. Daweritz, and K. H. Ploog, J. Phys. D **38**, A169 (2005).
[16] D. Anderson, J. B. Goh, and J. A. Dinglasan, "Nanoparticles confined in polyelectrolytes," U.S. Patent No. 7501180 (11 March 2009).
[17] D. Sarid, *Scanning Force Microscopy: With Applications to Electric, Magnetic, and Atomic Forces* (Oxford University Press, New York, 1993).